

## GOLD NANOSTRUCTURES SPUTTERED ON ZINC OXIDE THIN FILM AND CORNING GLASS SUBSTRATES\*

Ondrej Szabó<sup>1</sup>, Soňa Flickyngerová<sup>1</sup>, Teodora Ignat<sup>2,3</sup>, Ivan Novotný<sup>1</sup>,  
Vladimír Tvarožek<sup>1</sup>

<sup>1</sup>Institute of Electronics and Photonics, Faculty of Electrical Engineering and Information  
Technology, Slovak University of Technology, Bratislava, Slovakia

<sup>2</sup>Institute of Analytical Chemistry, Faculty of Chemical and Food Technology, Slovak  
University of Technology, Bratislava, Slovakia

<sup>3</sup>Laboratory of Nanobiotechnology, IMT-Bucharest, Bucharest, Romania

**Abstract.** *Forming of Au nanostructures on Corning glass substrates and transparent conductive oxide ZnO:Al thin films by the RF diode sequential sputtering is presented. The morphology of Au structures was analysed by scanning electron microscopy (SEM) with the free ImageJ software, the optical properties were evaluated by UV-Vis spectrometry and micro-Raman spectroscopy. The sputtering power density (deposition rate) and nominal Au thickness caused changes in the sizes (10 – 1000 nm<sup>2</sup>) and nearest neighbour NN distances (4 – 40 nm) of Au nanostructures. The morphology of nanostructures exhibited the LogNormal distribution of the size of nanostructures. The lowest sputtering power density/deposition rate (9 mW/mm<sup>2</sup>/0.12 nm s<sup>-1</sup>) was optimal to get both the high optical transparency and a superior activity surface-enhanced Raman scattering of 11-mercaptoundecanoic acid adsorbed on the Au/ZnO:Al film.*

**Key words:** *Sputtering, ZnO:Al thin films, Au nanostructures, plasmon absorption, surface-enhanced Raman scattering*

### 1. INTRODUCTION

Developing the approaches for obtaining nanostructures consisting of noble metals with complete control over the shape of surface structures remains a major challenge. In fact, the real objective is to produce small objects with reproducibly matching the requirements of the specific applications in photonics, biosensors, electronics, nanofluidics and other emerging fields. At ‘nano’ level a variety of interesting optical and plasmonic

---

Received September 16, 2014; received in revised form August 27, 2015

**Corresponding author:** Ondrej Szabó

Institute of Electronics and Photonics, Faculty of Electrical Engineering and Information Technology,  
Slovak University of Technology, Ilkovičova 3, SK-812 19 Bratislava, Slovakia  
(e-mail: ondrej.szabo@stuba.sk)

\*An earlier version of this manuscript received the Best Oral Paper Award at the 29<sup>th</sup> International Conference on Microelectronics (MIEL 2014), Belgrade, 12-15 May, 2014 [1].

effects occur. Creating ‘hot spots’ which typically reside in interstitial voids of metal nanoparticles and metal structures with intersections, bifurcations and high radius of curvatures gives rise to peaks in the light absorption spectra of the materials and are believed to be primarily responsible for the huge amplifications seen in single molecule SERS (Surface Enhanced Raman Spectroscopy). To construct a SERS active substrate, a variety of architectures have been developed [2, 3]. Most of the published papers present SERS substrates constructed from metal aggregates, such as Au and Ag layers with different shapes and sizes, dependent of the Raman wavelength [4]. It is important to notice that a SERS active nanostructure can act as a reporter for biological assays in the same manner as fluorescent or radioactive reporters with mentioned advantages. SERS is a fascinating process by which normally weak Raman signals can be amplified by many orders of magnitude. Among nanostructured noble metals, gold (Au) has a special importance because of its stability and unique electrochemical and optical properties. Gold nanostructures are often prepared by two approaches: (i) ‘top-down’ approach in which bulk materials are made into micro/nano structures with the help of downscaling techniques (lithographic techniques) and (ii) ‘bottom-up’ approach, where small building blocks are assembled into bigger structures (like electrochemical deposition, sputtered micro-/nano- structures) [5, 6, 7, 8]. Therefore, a lot of effort has been dedicated to gold nanostructures, mainly due to their exciting applications as substrates for SERS [9], catalysis [10], biomolecular and DNA sensors [11], super-hydrophobicity/hydrophilicity substrates [12], selective solar absorbers, antireflection coatings or diffraction gratings [13].

Zinc oxide (ZnO) is an n-type semiconductor with a wide band gap (3.3 eV at 300 K) used as a promising candidate to replace other wide band gap semiconductors, such as indium tin oxide (ITO) [14]. This material is used as a transparent electrode in optoelectronic devices. It has been found that the conductivity of ZnO films increases when doped with aluminium, Fig. 1a. ZnO doped by Al (ZnO:Al) used as transparent conduction oxide (TCO) films have attracted attention due to their nontoxic nature, cost-effectiveness and easy fabrication. However, a sensor based on ZnO:Al still has some limitations. Sensor sensitivity can be improved by several techniques, such as preparing the sensor material in a nanostructure or adding a noble metal. Definitely, it is still needed to create hybrid nanostructures by combining two or more constituents due to their unique composition-dependent properties that are very hard to reach by just one material [6].

The purpose of our study was to develop and optimize technology which results in the formation of Au nanostructures on TCO ZnO:Al thin film/Corning glass substrates by RF diode sputtering. The obtained structure was characterized by scanning electron microscopy (SEM) and by optical spectrometry in order to have a deep and complete view of the developed nanostructured substrates.

The study is divided into different directions focused on creating and characterizing the Au nanostructures/ZnO:Al thin films: (i) ZnO:Al thin films characterization - their crystalline structure, electrical properties and their electrochemical response by the cyclic voltammetry; (ii) the influence of the RF diode sputtering power on the morphology of ultra-thin gold layers deposited on the ZnO:Al thin film and Corning glass substrates; (iii) surface plasmon absorption of Au/Corning glass and Au/ZnO:Al substrates; (iv) the SERS response of the Au/ZnO:Al substrate functionalized with 11-mercaptoundecanoic acid (11-MUA) [15].

## 2. EXPERIMENTAL

The RF diode sputtering system Perkin/Elmer 2400/8L for deposition of both ZnO:Al thin films and Au nanostructures was used. Continuous sputtering ZnO:Al thin film was performed by the standard static mode of deposition (the substrates were placed under the target) using a ceramic target (ZnO+2 wt. % of Al<sub>2</sub>O<sub>3</sub>) in Ar working gas. Post-deposition annealing of ZnO:Al thin films with a thickness of 560 nm was conducted at 500 °C for 30 min in the forming gas N<sub>2</sub>:H<sub>2</sub> (90:10). Their crystallographic orientation was analysed by X-ray diffractometer X'Pert Pro with a Bragg-Brentano goniometer equipped with an ultra-fast linear semiconductor detector PIXcel and Copper K $\alpha$  radiation source ( $\lambda = 0.154$  nm). Electrical properties of ZnO:Al thin films were estimated by Hall measurements.

Deposition of Au was performed by the sequential (dynamic) mode of sputtering [16]: Au target of 102.4 mm in diameter, Ar pressure of 1.3 Pa. The substrates were in motion under the target by turning the substrate holder. The deposition time corresponding to one turn was approx. 9 seconds. Corning glass substrates (bare or covered by TCO ZnO:Al thin film) were heated to a temperature of 200 °C before Au deposition. The influence of RF power on the morphology of Au nanostructures was examined. The sputtering rates were determined from the thicknesses and time of deposition of homogeneous thin films, which were evaluated by a Dektak profilometer. The amount of sequentially sputtered material was estimated by the nominal thickness of the film deposited during one-turn period ( $\approx 9$  s) under the target. The sputtering rates of Au depended on the RF power density and they were 0.12 nm/s (9 mW/mm<sup>2</sup>), 0.25 nm/s (18 mW/mm<sup>2</sup>), 0.5 nm/s (36 mW/mm<sup>2</sup>) and 1.0 nm/s (72 mW/mm<sup>2</sup>).

After deposition of gold on ZnO:Al/Corning glass substrate, the samples were subsequently transferred to 11-mercaptoundecanoic acid 2  $\mu$ mol/ml solution for 24 h, this molecule being well known for its ability to bond on gold surfaces. In order to remove the physically absorbed 11-MUA molecule, all samples were rinsed with ethanol and water and dried in nitrogen. All chemicals were used as received without further purification.

The morphology of Au structures was characterized by scanning electron microscopy (SEM) JEOL 7500F, their optical transparency was measured by AVA Spec 2048 Fiber Optic Spectrometer. Micro Raman spectra of the samples were obtained using a Spectroscopy&Imaging MonoVista UV-VIS-NIR confocal Raman Microscope using a visible 514 nm laser. It can calculate the area and the nearest neighbour (NN) distance of objects specified in pixels, pixel value statistics of user-defined selections and creates density histograms and line profile plots. It supports standard image processing functions, such as contrast manipulation, sharpening, smoothing, edge detection and median filtering. The size (area) of nanostructures (islands) is characterized by the area of selection in square pixels. Original SEM images (size of 1280 $\times$ 1024 pixels) were cropped for evaluation to a size of 640 $\times$ 512 pixels.

## 3. RESULTS AND DISCUSSION

For evaluation of surface morphologies we used SEM and the image processing program ImageJ which is an open source program [17]. Examples of SEM image processing are given in Figs. 1, 2, 3, 4. Statistical analysis of SEM images showed the Poisson (LogNormal) distribution of the size of surface grains and nanostructures, and their NN distances exhibited a Gaussian distribution. The modus is the value that appears most often in a set of data (Fig. 4).

The growth of nanostructures, i.e., also their morphology, was influenced by the type of substrate: polycrystalline textured ZnO:Al thin film on Corning glass or amorphous Corning glass.

The 560 nm thick ZnO:Al film was polycrystalline with preferred (002) orientation [18]. The structural columnar hierarchy of the continuous sputtered ZnO:Al film is shown in Fig. 1b. Crystalline structures of the film were corresponding to zone 2 of the crystalline structure of our zone representation [19]. Continuous sputtering generally led to the growth of bigger columnar grains in comparison with sequential sputtering. This effect was particularly caused by self-heating of the growing film during sputtering and by an increase of the deposition time (larger thickness). It showed the evolution of column-shaped structures during the growth (the so-called V-shape growth), Fig. 1c. A similar grain hierarchy was observed in both experimental results and theoretical simulations [20]. The size of columnar grains oriented perpendicularly to the substrate was increased in the direction to surface, top areas of the grains in the surface plane were characterized by LogNormal distribution with modulus  $1050 \text{ nm}^2$  and the modulus of NN grain distances was 65 nm (Fig. 1d). Crystalline columnar structure of AZO film had an influence on their electrical properties obtained by Hall measurements. Relatively high resistivity ( $1 \times 10^{-2} \Omega \text{ cm}$ ) was caused by low electron mobility ( $2.5 \text{ cm}^2/\text{Vs}$ ) at electron concentration  $2 \times 10^{20} \text{ cm}^{-3}$ . If one supposes the electron grain-boundary scattering, the calculated value of the electron mean free path [20] is 30 nm. The ionized impurity scattering is getting dominant in the range of electron concentrations greater than  $10^{20} \text{ cm}^{-3}$  according to behaviours of degenerate semiconductors [21].

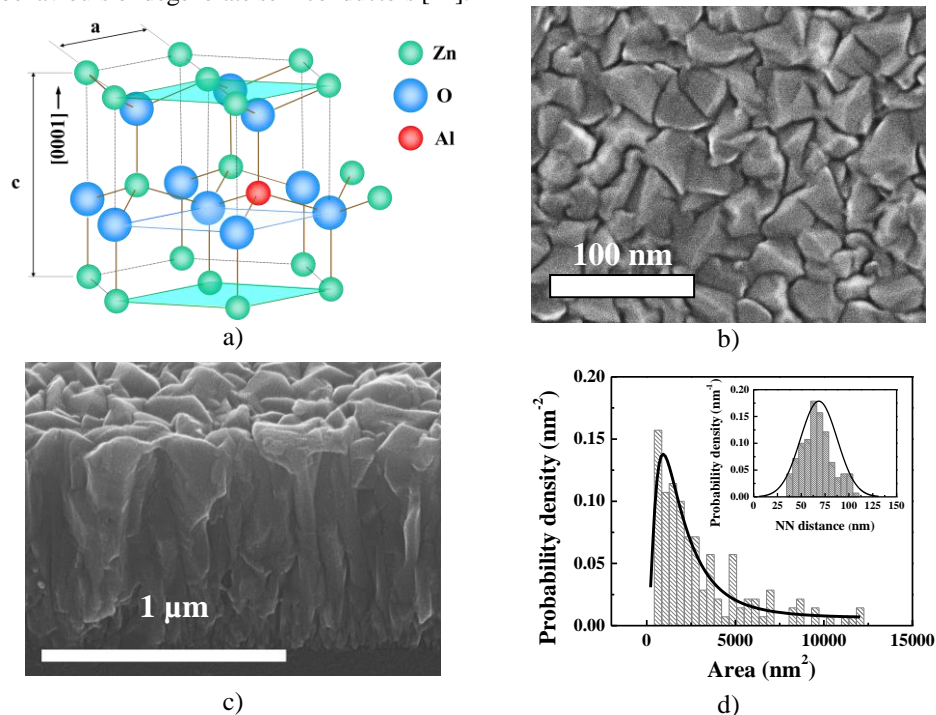


**Fig. 1** Schematic representation of the wurtzite ZnO structure doped by Al (AZO) (a), surface SEM images and cross-section (b), (c) and SEM image processed results (histograms) (d) of continuous sputtered ZnO:Al thin films.

In comparison with continuous sputtering, the sequential mode of sputtering allows to achieve very low deposition rates, higher homogeneity and well-controllable 3- dimensional coverages [15].

For the growth of Au nanostructures the early stages of thin film growth are important: nuclei formation, growth of clusters and islands and their coalescence [22]. SEM images of Au nanostructures sputtered on Corning glass are in Fig. 2. The power density was changed from  $18 \text{ mW/mm}^2$  to  $72 \text{ mW/mm}^2$ . This resulted in increasing the modulus of nanostructure (island) areas from  $50 \text{ nm}^2$  to  $600 \text{ nm}^2$  (Fig. 4). Simultaneously, the modulus of the nearest neighbour distances of islands increased from  $11 \text{ nm}$  to  $34 \text{ nm}$ .

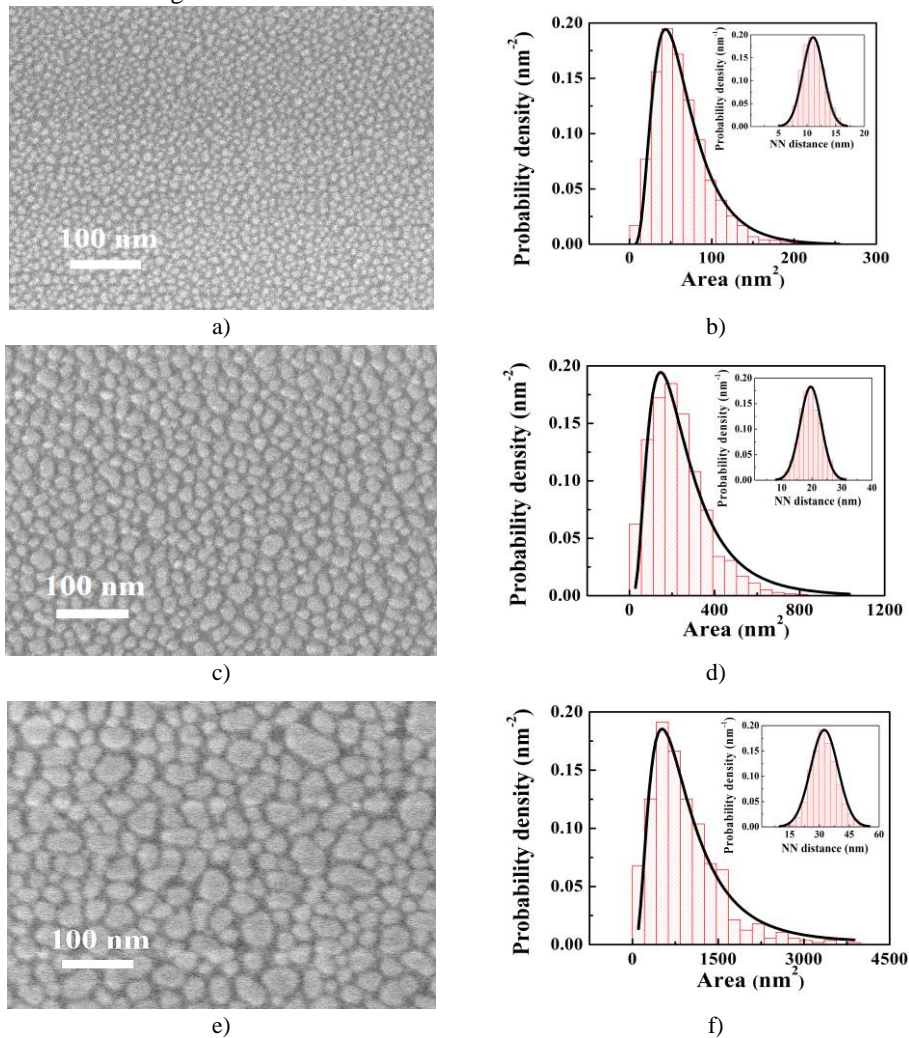


**Fig. 2** SEM images of Au nanostructures sputtered on Corning glass substrate at different ratios power density/deposition rate/nominal thickness: a)  $18 \text{ mW/mm}^2 / 0.25 \text{ nm s}^{-1} / 2.2 \text{ nm}$ , c)  $36 \text{ mW/mm}^2 / 0.5 \text{ nm s}^{-1} / 4.5 \text{ nm}$ , e)  $72 \text{ mW/mm}^2 / 1 \text{ nm s}^{-1} / 9 \text{ nm}$ . b), d), f) Corresponding size and NN distance distribution of Au nanostructures.

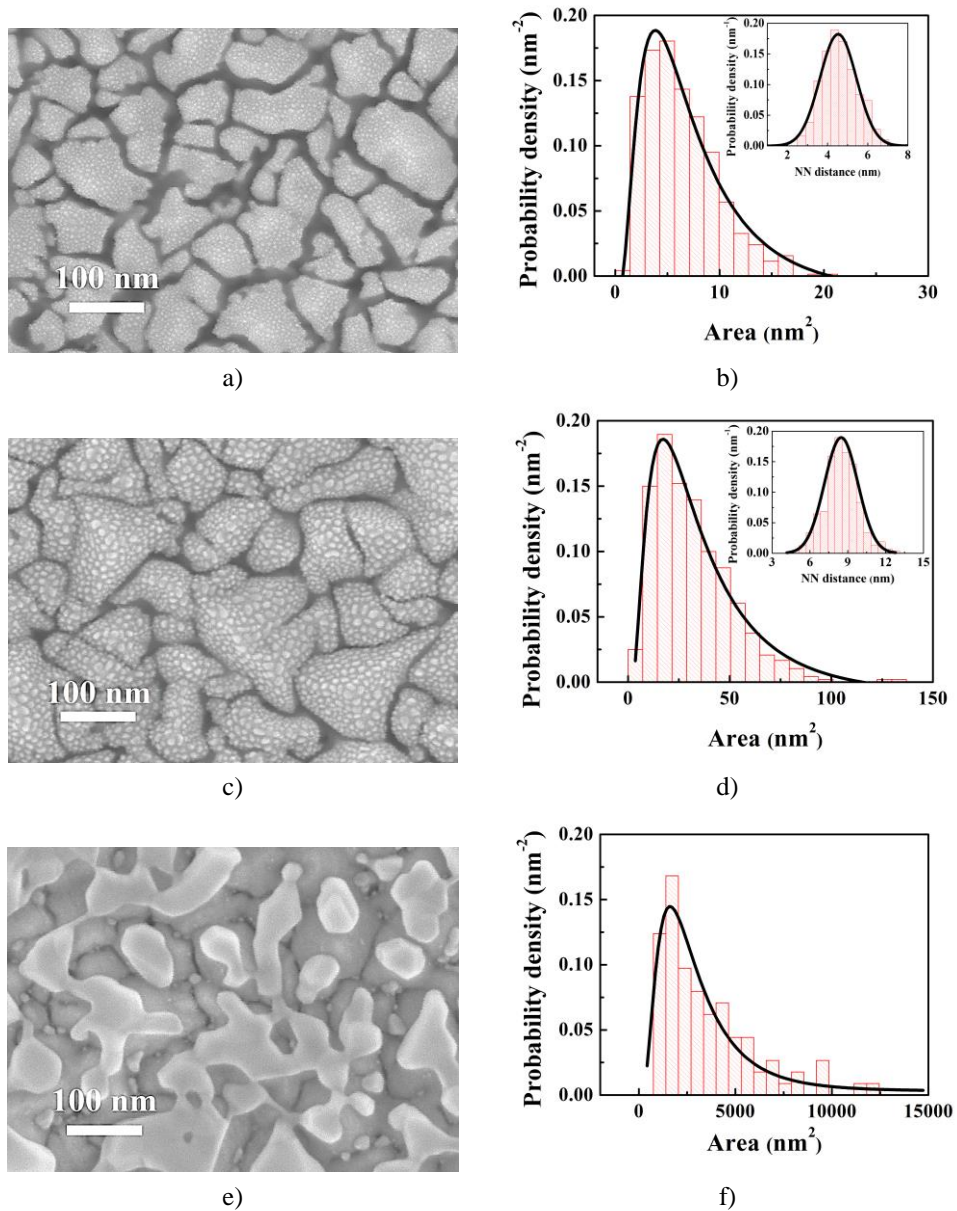


**Fig. 3** SEM images of Au nanostructures sputtered on ZnO:Al thin film / Corning glass substrate at different ratios power density / deposition rate / nominal thickness: a)  $9 \text{ mW/mm}^2 / 0.12 \text{ nm s}^{-1} / 1.1 \text{ nm}$ , c)  $18 \text{ mW/mm}^2 / 0.25 \text{ nm s}^{-1} / 2.2 \text{ nm}$ , e)  $72 \text{ mW/mm}^2 / 1 \text{ nm s}^{-1} / 9 \text{ nm}$ . b), d), f) Corresponding size and NN distance distribution of Au nanostructures.

The orphology of Au nanostructures formed on ZnO:Al thin film was affected by the power density from  $9 \text{ mW/mm}^2$  to  $72 \text{ mW/mm}^2$  as well as by the polycrystalline texture nature of the film surface (Fig. 3). The modus of Au nanostructure areas on ZnO:Al thin film increased from  $5 \text{ nm}^2$  to  $20 \text{ nm}^2$  and the modus of NN distance distribution was changed from  $4 \text{ nm}$  to  $9 \text{ nm}$  (Fig. 4).

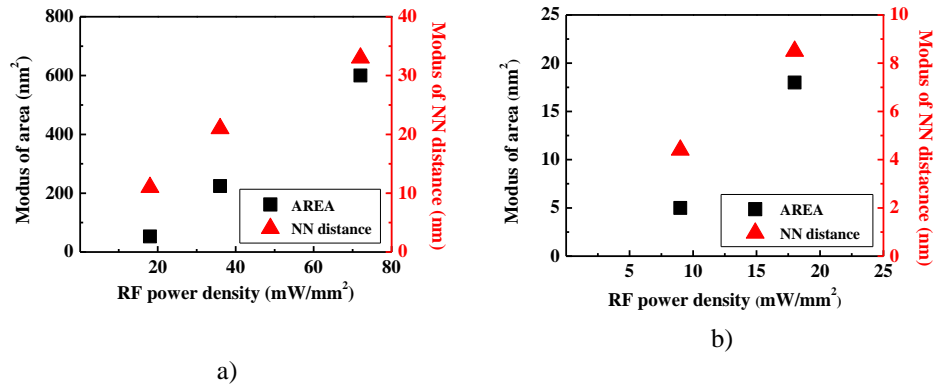


**Fig. 4** Modus of Au nanostructure areas and NN distance distribution sputtered on Corning glass / ZnO:Al thin film.

Characteristic features of the morphology of RF diode sputtered Au nanostructures as well as another behaviour of them are comparable with the results obtained by DC diode sputtering [6, 23]. Spectral optical transmittances of an uncoated ZnO:Al / Corning glass substrate covered by Au at different power densities are shown in Fig. 5. The range of power densities corresponded to the nominal thickness interval  $1.1 \leq d_{\text{Au}} \leq 9 \text{ nm}$ . Transmittance of ZnO:Al film / Corning glass substrate ( $\sim 90 \%$ ) decreased down to  $\sim 50 \%$  with an increase of sputtering power densities (i.e., also with Au nanostructure sizes).

The minimum in optical transmittance curves corresponds to surface plasmon absorption [23] caused by collective oscillation of electrons on the surfaces covered by Au nanostructures (Fig. 5a, b). Sputtering power densities had an influence on the surface plasmon absorption wavelengths which varied in the range from  $572 \text{ nm}$  to  $626 \text{ nm}$  (corresponding plasmon resonant frequencies were  $524 \text{ THz}$  to  $479 \text{ THz}$ ). Surface plasmon absorption peaks are characteristic for Au nanostructures. This is in agreement with Au nanoparticles prepared by DC sputtering technologies [24]. The change of the shape of the plasmon absorption curves and the shift of plasmon resonant frequencies with the sputtering power were caused by the different sizes of Au nanostructures and their various separations [23]. The red-shift of the absorption minimum with an increase of nominal thicknesses from  $1.1 \text{ nm}$  up to  $9 \text{ nm}$  (Fig. 5 a) was not too strong, as reported in [3]. The use of thin film ZnO:Al under Au nanostructures suppressed the surface plasmon resonance (Fig. 5 b) because the higher roughness of the ZnO:Al surface (in comparison with a glass surface) influenced this effect.

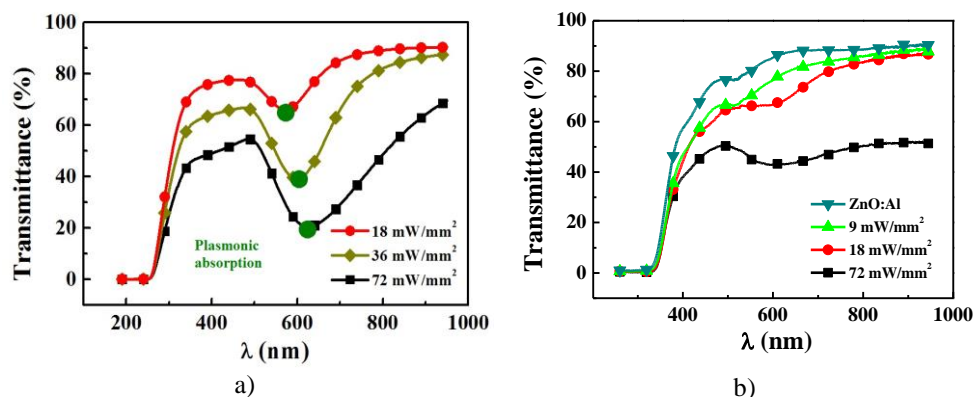


**Fig. 5** Spectral transmittance of Au nanostructures sputtered at different power densities: a) On Corning glass substrate, b) on ZnO:Al thin film / Corning glass substrate.

ZnO thin films and nanostructures have several unique advantages (such as high surface area, nontoxicity, good biocompatibility and high electron communication features) for the development of electrochemical biosensors [25, 26]. Zinc oxide exhibits a large isochemical point ( $ISE \approx 9.5$ ), thus electrostatic attachment of bio-substances (e.g. proteins) with low ISE ('negative charged') is very easy [27]. It is very important to note that ZnO thin films are relatively stable around a neutral pH 7 and this gives ZnO-based sensors much more biocompatibility in biological fluids and species [28], since most of the biological fluids are around pH of 7 (e.g., blood has pH 7.4 [29]) Therefore in electrochemical experiments we used a 0.1 M KCl solution whose properties are partly similar to blood. Preliminary electrochemical behaviour of ZnO:Al was controlled by cyclic voltammetry (Fig. 6). Cyclic voltammetry of ZnO:Al thin film chips was performed using a Ag/AgCl reference electrode at a scan rate of 100 mV/s. Two current peaks at  $-1200$  mV and  $-1600$  mV correspond to redox reactions on the ZnO:Al electrode [22]. A relative wide potential window with allow detecting a number of bio- / inorganic species including heavy metals [30].

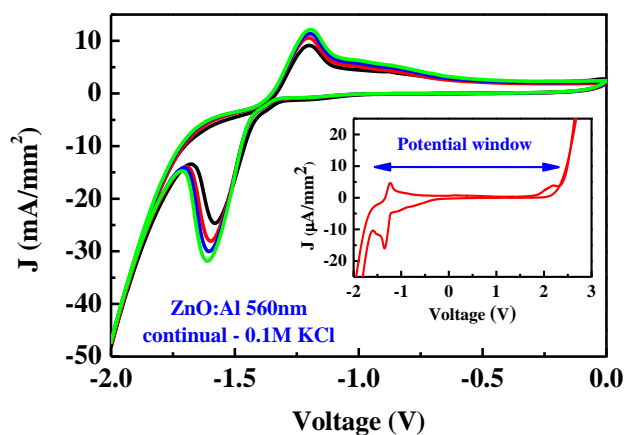


**Fig. 6** Cyclic voltammogram of ZnO:Al film of thickness 560 nm.



Self-assembly of monolayers of 11-mercaptoundecanoic acid [30] on surfaces of gold nanostructures sputtered on ZnO:Al thin film has been investigated by Surface Enhanced Raman Spectroscopy. The measured vibration bands of 11-MUA using Raman microscopy and their mode assignments can be attributed to bands which give information about the adsorption of 11-MUA on gold, surface  $\nu(\text{C-S})$  gauche at  $652\text{ cm}^{-1}$ ,  $\nu(\text{C-S})$  trans at  $700\text{ cm}^{-1}$ ,  $\nu(\text{C-C})$  at  $1058\text{ cm}^{-1}$ ,  $\nu_s(\text{COO-Au})$  at  $1394\text{ cm}^{-1}$ . Both apparent assignments of  $\nu(\text{C-S})$ T and  $\nu(\text{C-C})$  give information about the conformational state of the adsorbed molecule on the gold surface, showing the trans nature of the adsorbed molecule. Moreover, it was observed that the peak intensity of adsorbed 11-MUA on Au nanostructures, when exposed to  $9\text{ mW/mm}^2$  power density, is significantly superior to other exposed substrates (Fig. 7). It is known that the Raman signal strength is proportional to the power of the Raman laser exciting the sample. In our case a decrease in the intensity of major Raman peaks was observed even when the laser power was increasing. This can be explained by damaging the sample with increasing the laser power. Further, it was observed that the substrate without Au nanostructures did not have the specific Raman bands of the organic molecule. Impressive enhancements are obtained when an organic molecule is adsorbed on a nanostructured substrate like Au, Ag, Pt [24, 31, 32, 33, 34].

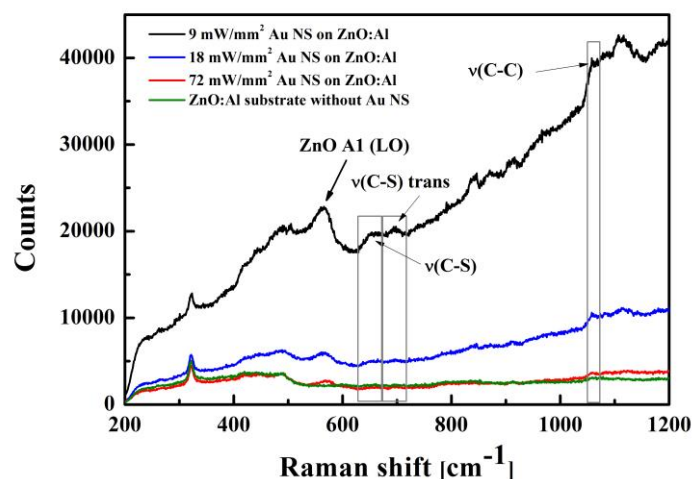


**Fig. 7** SERS spectra of 11-MUA on Au nanostructures (NS) / ZnO:Al thin film at different Au sputtering power densities.

#### 4. CONCLUSION

Crystalline textured and columnar structure of ZnO:Al film influenced their electrical properties but the acquired resistivity ( $1 \times 10^{-2}\ \Omega\text{ cm}$ ) was sufficient to perform the cyclic voltammetry measurements. Preliminary results of electrochemical properties of sputtered ZnO:Al thin films having the columnar crystalline structure, particularly nanotextured one, have confirmed their potential for the future application in biochemical sensors [35].

Presented results have confirmed the ability of RF diode sputtering to prepare gold nanostructures of variable morphologies by changing the RF power density. Sequential

mode of sputtering seems to be a well-controllable and precise technology with low deposition rate in the range from 0.1 to 1 nm s<sup>-1</sup>. The crystalline structure of sequentially sputtered films became generally less-dense containing voids, gas interstitials and vacancies. This porous structure is caused by the interrupted type of sequential deposition. It allows easier formation and reshaping of nanostructures by post-deposition annealing [36]. The outputs of our research have verified the possibility of Au surface plasmon forming by sequential sputtering without using masks and lithography. An apparent shift of the plasmon absorption minimum to longer wavelengths was observed. It was caused by an increase of the nominal thicknesses from 1.1 nm up to 9 nm. Sputtering of gold on ZnO:Al thin film substrate is a very simple and low cost technique for generating different gold morphologies and nanostructures. Our substrate was based on ZnO because its high refractive index promotes strong light confinement, hereby increasing the SERS effect [24]. In addition, the lack of toxicity and high chemical stability of ZnO make it a prospective material in biomolecule detection application.

By varying the experimental conditions (RF power of deposition), the surface with nanostructures has been modified with 11-mercaptoundecanoic acid molecule and observed as a fingerprint of the molecule by Raman spectroscopy. The organic molecules deposited on sputtered gold at RF power density 9 mW/mm<sup>2</sup> have better features than the other prepared substrates. The first results are interesting and show an encouraging, easy way to obtain an analytical tool for molecule Raman detection.

The research of Au nanostructures sputtered on both glass and columnar TCO ZnO:Al thin films is going on because its outputs are applicable in biochemical sensors.

**Acknowledgement:** *The presented work was supported by the SK VEGA Project 1/0459/12 and by the Competence Center for SMART Technologies for Electronics and Informatics Systems and Services, ITMS 26240220072, funded by the R&D OP Programme ERDF SR. This work was supported also by the Scientific Grant Agency VEGA of the Slovak Republic (Project No 1/0361/14) and the National Scholarship Programme of the Slovak Republic (Dr. Teodora Ignat). We thank Dr. J. Kováč jr. for Raman measurements and Dr. P. Šutta for XRD analyses.*

## REFERENCES

- [1] O. Szabo, S. Flickyngerova, V. Tvarozek, and I. Novotny, "Sputtered Gold Nanostructures", In Proceedings of the International Conference on Microelectronics (MIEL 2014), Belgrade, 12-15 May, 2014, pp. 245-248.
- [2] S. Bhavya, R. R. Frontiera, A. I. Henry, E. Ringe, R. P. van Duyne, "SERS: Materials, applications, and future", *Materials Today*, 2012, 15, pp. 16-25.
- [3] S. Mahajan, T. Hutter, U. Steiner and P. G. Oppenheimer, "Tunable Microstructured Surface-Enhanced Raman Scattering Substrates via Electrohydrodynamic Lithography", *J. Phys. Chem. Lett.* 2013 (4), pp. 4153-4159.
- [4] H. W. Cheng, S. Y. Huan, R. Q. Yu, "Nanoparticles-based substrates for surface-enhanced Raman scattering of bacterial spores", *Analyst*, 2012, 137, pp. 3601-3608.
- [5] J. Elias, M. Gizowska, P. Brodard, R. Widmer, Y. deHazan, T. Graule, J. Michler and L. Philippe, "Electrodeposition of gold thin films with controlled morphologies and their applications in electrocatalysis and SERS", *Nanotechnology*, 2012, vol. 23, 255705.
- [6] J. Siegel, O. Lyutakov, V. Rybka, Z. Kolska, V. Svorcik, "Properties of gold nanostructures sputtered on glass", *Nanoscale Research Letters* 2011, 6:96, 9 p.

- [7] R. Alvarez, J. M. García-Martín, M. Macías-Montero, L. Gonzalez-Garcia, J. C. González, V. Rico, J. Perlich, J. Cotrino, A R González-Elipiel and A. Palmero, "Growth regimes of porous gold thin films deposited by magnetron sputtering at oblique incidence : from compact to columnar microstructures", *Nanotechnology*, 2013, vol. 24, 045604, 9 p.
- [8] P. Lansaker, "Gold-Based Nanoparticles and Thin Films: Application to Green Nanotechnology", Dissertation, *Acta Universitatis Upsaliensis*, Uppsala, ISBN 978-91-554-8420-0, 2012, 100 p.
- [9] K. Kneipp, Y. Wang, H. Kneipp, L. T. Perelman, I. Itzkan, R. R. Dasari, and M. S. Feld, "Single Molecule Detection Using Surface-Enhanced Raman Scattering (SERS)", *Phys. Rev.*, 1997, Lett. 78, pp 1667.
- [10] T. Fujita, P. Guan, K. McKenna, X. Lang, A. Hirata, L. Zhang, Tt Tokunaga, S. Arai, Y. Yamamoto, N. Tanaka, Y. Ishikawa, N. Asao, Y. Yamamoto, J. Erlebacher and M. Chen, "Atomic origins of the high catalytic activity of nanoporous gold", *Nature Mater*, 2012, 11, pp. 775-780.
- [11] J. H. Kim, T. Kang, S. M. Yoo, S. Y. Lee, B. Kim and Y.-K. Choi, "A well-ordered flower-like gold nanostructure for integrated sensors via surface-enhanced Raman scattering", *Nanotechnology*, 2009, 20, 235302 (6pp).
- [12] X. Yu, Z. Q. Wang, Y. G. Jiang, F. Shiand X. Zhang, "Reversible pH-Responsive Surface: From Superhydrophobicity to Superhydrophilicity", *Adv.Mater*, 2005, 17, pp. 1289-1293
- [13] A. S. Dimitrov, K. Nagayama, "Continuous Convective Assembling of Fine Particles into Two-Dimensional Arrays on Solid Surfaces", *Langmuir*, 1996, 12, pp. 1303-1311.
- [14] C. F. Klingshim, A. Waag, A. Hoffmann, J. Geurts, *Zinc Oxide - From Fundamental Properties Towards Novel Applications*, Springer, 2010.
- [15] L. Sun, D. Zhao, M. Ding, H. Zhao, Z. Zhang, B. Li, D. Shen, "A white-emitting ZnO-Au nanocomposite and its SERS applicant", *Applied surface science*, 2012, 258, pp. 7813-7819.
- [16] I. Novotny, V. Tvarozek, P. Suta, M. Netrvalova, J. Novak, I. Vavra, P. Elias, "Preparation of Shell Nanocrystalline Ga-doped ZnO Ultra-Thin Films by Sputtering", In Proceedings of 28th Int. Conf. on Microelectronics, Nis, Serbia and Montenegro, 2012.
- [17] ImageJ website: <http://imagej.nih.gov/ij/>, (2013).
- [18] V. Tvarozek, P. Suta, S. Flickyngerova, I. Novotny, P. Gaspierik, M. Netrvalova, E. Vavrinsky, "Preparation of transparent conductive AZO thin films for solar cells", *Semiconductor Technologies*, Chapter 12, (2010), pp. 271-294.
- [19] V. Tvarozek, I. Novotny, P. Sutta, S. Flickyngerova, K. Shtereva, E. Vavrinsky, "Influence of Sputtering Parameters on Crystalline Structure of ZnO Thin Films", *Thin Solid Films* 515 (2007), pp. 8756-8760.
- [20] Y.D. Fan, X. P. Li, J. Yang, J. P. Li, "Microscopic Model for Columnar Growth of Thin Films", *Phys. Stat. Sol. (a)*, 134 (1992), pp. 157-166.
- [21] J. G. Lu, Z. Z. Ye, Y. J. Zeng, L. P. Zhu, L. Wang, J. Yuan, B. H. Zhao and Q. L. Liang, "Structural, optical, and electrical properties of (Zn, Al)O films over a wide range of compositions", *J. of Appl. Physics* 100, (7), 2006, 073714.
- [22] R. Renuka, I. Skrivinasan, S. Ramamurthy, A. Veluchamy, N. Venkatakrishnan, "Cyclic voltammetry study of zinc oxide electrodes in 5.3 M KOH", *Journal of Applied Electrochemistry* 31, 2001, pp. 655-661.
- [23] J. Siegel, O. Kvitek, O. Lyutakov, A. Reznickova, V. Svorcik, "Low pressure annealing of gold nanostructures", *Vacuum*, Vol. 98, pp. 100-105.
- [24] T. Ignat, M. A. Husanub, R. Munozc, M. Kuskoa, M. Danilaa, C. M. Teodorescub, "Gold nano-island arrays on silicon as SERS active substrate for organic molecule detection", *Thin solid Films*, 2014, 550, pp. 354-360.
- [25] P. Singh, Sunil K. Arya, P. Pandey, B. D. Malhotra, "Cholesterol biosensor based on rf sputtered zinc oxide nanoporous thin film", *Appl. Phys. Lett.* 91 (2007) 063901.
- [26] X. You, J. H. Pikul, W. P. King, J. J. Pak, "Zinc oxide inverse opal enzymatic biosensor", *Applied Physics Letters* 102, 253103, 2013, doi. 10.1063/1.4811411 S.
- [27] E. Topoglidis, A. E. G. Cass, B. O' Regan, J. R. Durrant, "Immobilization and bioelectrochemistry of proteins on nanoporous TiO<sub>2</sub> and ZnO films", *Journal of Electroanalytical Chemistry* 517 (2001), pp. 20-27.
- [28] J. Zhou, N. Xu and Z. L. Wang, "Disolving Behavior and Stability of ZnO Wires in Biofluids: A study on Biodegradability and Biocompatibility of ZnO Nanostructures", *Adv. Mater.* 2006, 18, pp. 2432-2435.
- [29] H. J. Park and S. Mho: "Electrochemical Impedance Spectroscopy and Voltammetry of Zinc in Dilute Alkaline Solutions". *Analytical Sciences* Vol.13 Supplement (1997), pp. 311-316.
- [30] J. Wang, "Analytical electrochemistry", Wiley-Vch. 2006.
- [31] S. A. MAIER, "Plasmonics: Fundamentals and Applications", Springer, New York, 2007. 223 p.

- [32] J. L. Hammond, N. Bhalla, S. D. Rafiee and P. Estrela, “Localized Surface Plasmon Resonance as a Biosensing Platform for Developing Countries”, *Biosensors* 2014, 4(2), pp. 172-188.
- [33] Y. Cao, D. Li, F. Jiang, Y. Yang and Z. Huang, “Engineering Metal Nanostructure for SERS Applications”, *Journal of Nanomaterials*, 2013, pp. 1238 (12).
- [34] O. Szabo, S. Kovacova, J. Skriniarova, D. Rossberg, V. Tvarozek, “Effect of annealing on properties sputtered Au nanostructures”, *ADEPT 2015*, pp. 120-123.
- [35] C. Ratscha, J.A. Venable, “Nucleation theory and the early stages of thin film growth”, *J. Vac. Sci. Technol. A* 21(5) (2003), pp. 96-109.
- [36] J. Siegel, O. Kvitek, P. Slepicka, J. Nahlik, J. Heitz, V. Svorcik, “Structural, electrical and optical studies of gold nanostructures formed by Ar plasma-assisted sputtering”, *Nuclear Instruments and Methods in Physics Research B* 272 (2012), pp.193-197.